International Communications in Heat and Mass Transfer 167 (2025) 109375

Contents lists available at ScienceDirect

International Communications in Heat and Mass Transfer

journal homepage: www.elsevier.com/locate/ichmt

Modeling of freeze-drying of mare's milk taking into account cracks

Timur Bekibayev [a,b], Uzak Zhapbasbayev [a,b], Nurbibi Imanbayeva [a,c,*], Ayaulym Rakhmatulina [a,d]

[a] Department of Mechanical Engineering and Robotics, U. Joldasbekov Institute of Mechanics and Engineering, Shevchenko Str. 28, Almaty 050010, Kazakhstan
[b] Scientific and Production Laboratory "Modeling in Energy", Satbayev University, Satbayev Str. 2, Almaty, Kazakhstan
[c] Department of Mechanical Engineering, Satbayev University, Satbayev Str. 22, Almaty 050000, Kazakhstan
[d] Department of Automation and Robotics, Almaty Technological University, Tole Bi Str., Almaty 050000, Kazakhstan

ARTICLE INFO

Keywords:
Freeze drying
Mare's milk
Crack in the porous structure of the product

ABSTRACT

The article presents the results of calculations of sublimation drying of mare's milk without cracks in the porous structure of the product and taking into account the formation of a crack. In the case of a crack, the calculation was carried out taking into account the cracking of the product at 4:00 h and the change in the permeability of the porous body during crack formation. Stefan's problem of the mare's milk sublimation process is solved by the numerical phase field method. The calculations obtained the distributions of temperature, pressure and steam velocity, showing the development of the sublimation front in the porous structure of the product over time. Without a crack, the sublimation front spreads from top to bottom of the product almost uniformly along the length of the porous structure and is in agreement with the known data. When cracks form in the porous structure, the front disintegrates into semi-independent drying zones. The crack leads to a decrease in pressure at the sublimation front and draws in steam from the product in its vicinity. The calculations showed that the presence of a crack accelerates the process of sublimation drying of mare's milk.

1. Introduction

Sublimation drying, a non-stationary process of heat and mass transfer, includes the stages of material freezing, sublimation dehydration and vacuum desublimation. Mathematical modeling allows us to describe these interrelated stages of drying and to optimize the process.

In the paper [1], the authors propose a framework that covers freeze-drying kinetics, dryer design calculations, and optimization strategies. The emphasis is on energy efficiency determined with analytical and empirical methods for kinetic modeling, which lays the foundation for resource-saving technologies. In the paper [2], a numerical model using the finite difference method is presented to analyze the transient thermal conductivity in freeze-drying of skim milk. The model takes into account the moving sublimation front, radiative and convective boundary conditions, the results indicate higher sublimation rates at lower chamber pressures. The study highlights the ability of the model to predict temperature profiles and sublimation dynamics.

In [3], the authors extend their efforts to model the porous media structure of beef freeze-drying, including Knudsen flow and distributed sublimation fronts. This study highlights the effect of gas fraction isolation in porous media and the importance of capturing the width of the sublimation front, demonstrating agreement with experimental data. In [4], the focus shifts to the capabilities of the equipment, particularly in industrial-scale freeze-dryers. Using computational fluid dynamics (CFD), the study examines the turbulent effects on vapor flow at high sublimation rates, demonstrating the accuracy of the simulation results in determining equipment pressure limits and optimizing throughput. In [5], a comprehensive model for freeze-drying of irregularly shaped food products is presented. The study emphasizes the integration of complex physicochemical properties into simplified formulations, with an emphasis on heat transfer mechanisms. By considering microstructural changes during freezing and drying, the study links theoretical modeling to practical applications. Accelerated freeze-drying methods are studied in [6], where a temperature-dependent structure is developed to enhance the sublimation rate without compromising the integrity of the material. Using the Genocchi operational matrix method, the study confirms the benefits of variable-dependent thermophysical properties, which contribute to higher

* Corresponding author at: Department of Mechanical Engineering and Robotics, U. Joldasbekov Institute of Mechanics and Engineering, Shevchenko Str. 28, Almaty 050010, Kazakhstan.
E-mail address: imanbaevan@mail.ru (N. Imanbayeva).

https://doi.org/10.1016/j.icheatmasstransfer.2025.109375

Available online 27 July 2025
0735-1933/© 2025 Published by Elsevier Ltd.

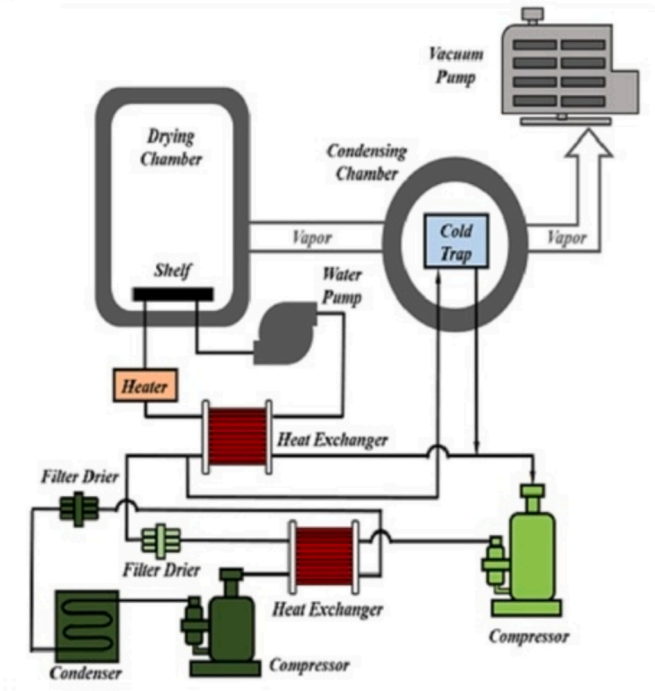


Fig. 1. Vacuum drying installation diagram.

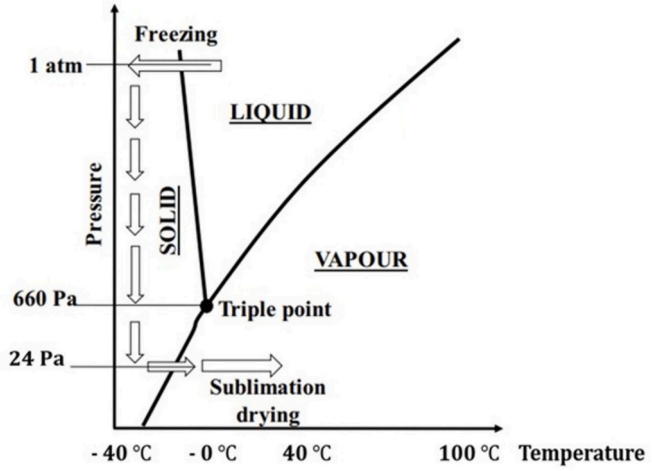


Fig. 2. Schematic diagram of sublimation of mare's milk.

drying rates and improved process efficiency.

In [7], a quasi-steady-state energy balance model is proposed to predict the multivariate kinetics of sublimation in peeled apple cubes. The inclusion of radiation and mass transfer coefficients in the model facilitates accurate prediction of the drying kinetics, making it a practical tool for scaling up operations. In [8], the Stefan-type heat and mass transfer problem with convection in pore regions is investigated. Analytical solutions show the influence of parameters such as Peclet and Lykov numbers on the sublimation dynamics. Graphical representations of the study provide valuable insights into the effects of the parameters, improving the understanding of sublimation processes.

The paper [9] examines convective heat and mass transfer in sublimation, considering parameters such as volumetric heat sources and Newtonian heat fluxes. The study shows that the inclusion of realistic heat fluxes accelerates sublimation processes, suggesting applications in energy storage and food technology. [10] uses a dynamic optimization approach to reduce energy consumption in freeze-drying processes for materials such as skim milk and instant coffee. The sequential quadratic programming method facilitates real-time optimization, balancing process efficiency with maintaining product quality.

The paper [11] discusses a Python-based modeling of freeze-drying kinetics with CFD gas dynamics simulations. This hybrid approach investigates drying rates dependent on vapor removal, highlighting the need for balanced condenser designs for uniform drying across all materials. The applications of CFD in freeze-dryer design are the focus of [12]. The study identifies geometry optimization and transient modeling, revealing critical aspects of freeze-drying equipment. This methodology improves process understanding and evaluates product drying and batch variance. [13] provides a detailed CFD analysis of pilot and large-scale freeze-drying chambers, focusing on valve and duct designs. The inclusion of dynamic modeling illustrates the potential for performance monitoring, contributing to improved industrial apparatus designs. This comprehensive review synthesizes ideas, highlighting advances in mathematical modeling, equipment design, and process optimization in freeze-drying technology. The papers collectively address critical issues in this area, paving the way for improved industrial applications.

In [14], a mathematical model is developed to analyze the exergy loss in the freeze-drying process and estimate the exergy loss during freezing, primary and secondary drying, steam condensation and vacuum pumping. The model includes dynamic factors to analyze the exergy loss at each stage. Using beef freeze-drying as an example, the results show that primary drying consumes 35.69 % of the total exergy, followed by steam condensation (31.76 %) and vacuum pumping (23.29%). Freezing and secondary drying account for only 3.56 % and 5.71 %, respectively. The study emphasizes that increasing the temperature of the cooling source in the steam condenser significantly reduces the total exergy loss. In addition, it indicates the optimum temperature.

In the paper [15], a new thermodynamically consistent numerical framework for modeling the three-dimensional sublimation process of ice at temperatures below the triple point and under low pressure conditions is developed. This framework introduces a new approach to describing the local thermodynamic equilibrium between frozen water (ice) and a mixture of water vapor and an inert gas with additional flexibility to account for anisotropic surface energy densities. The paper also proposes a new correlation for the diffusion coefficient of water vapor in nitrogen, obtained from equilibrium molecular dynamics simulations, which improves the accuracy of the model. In the paper [16], a comprehensive review of various continuous freeze-drying (lyophilization) concepts is presented with a main focus on their applications in the pharmaceutical industry.

It should be noted that all the above studies were carried out without the formation of cracks in the porous structure of the product.

The novelty of our work is the modeling of freeze-drying of mare's milk taking into account the formation of a crack in the porous structure of the product.

2. Physical model of the sublimation process

The physical model of the sublimation process is considered by means of a macroscopic description with continuous parameters in space and time (pressure, density, temperature, speed) [2,17–21]. Mare's milk is considered a liquid with the appropriate parameters. Although mare's milk contains water (89–91 %), protein (2–2.5 %), fats (1–1.5 %), lactose (6–7 %), etc. [18]. Skim mare's milk is poured into a tray measuring 50 × 40 cm and 7 mm high. The tray is placed on the shelves of a vacuum chamber of a typical installation, as in [17,18] (see Fig. 1).

In the first stage of the process, milk is frozen at atmospheric pressure from room temperature $T_1 = 30$ °C to temperature $T_2 = -40$ °C.

Fig. 2 shows a schematic diagram of the milk sublimation process in a vacuum chamber. It shows the transition of liquid milk into ice at a

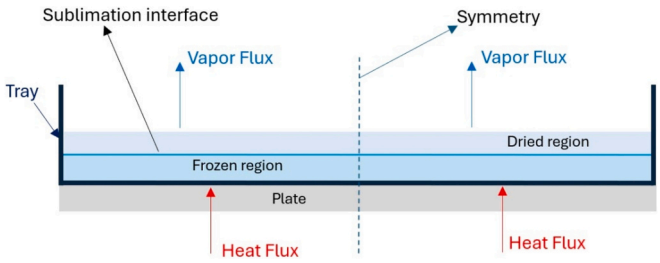


Fig. 3. Problem statement scheme.

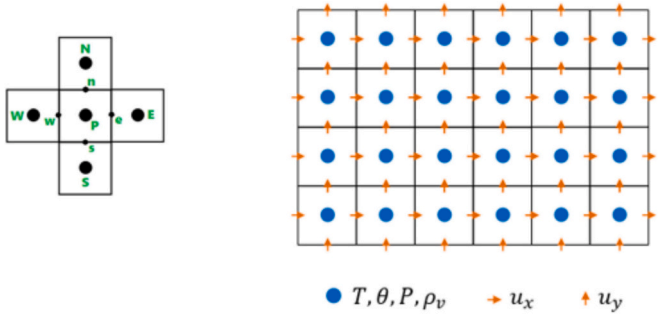


Fig. 4. Computational grid and designations of adjacent volumes and faces.

Table 1
Calculation parameters for sublimation of skim mare's milk.

Parameter name	Meaning	Units of measurement
Height of dishes	0.01	m
Length and width of dishes	0.5 x 0.4	m
Density of dry product	498	kg/m^3
Heat capacity of dry product	2595	J/(m °C)
Thermal conductivity of dry product	0.027	W/(m °C)
Porosity of drying product	0.709	units
Absolute permeability of dry product	$3.62 \cdot 10^{-10}$	m^2
Density of ice	913	kg/m^3
Heat capacity of ice	1967.8	J/(m °C)
Thermal conductivity of ice	2.1	W/(m °C)
Molar mass of steam	0.018	kg/mol
Heat capacity of steam	1674.7	J/(m °C)
Thermal conductivity of steam	0.025	W/(m °C)
Dynamic viscosity of steam	$8.36 \cdot 10^{-6}$	Pa·s
Latent heat of sublimation of ice	$2.7912 \cdot 10^6$	J/kg
Vacuum pressure in the drying chamber	24	Pa
Initial temperature of the frozen product	-40	°C
Temperature of the heating shelf	−10	°C
Temperature of the chamber	10	°C
Heat transfer coefficient between the chamber and the product	3.6	W/(m^2 °C)
Heat transfer coefficient between the shelf and the product	30	W/(m^2 °C)

pressure of 1 atm. In the ice state, the pressure in the vacuum chamber decreases from 10^5 Pa to 24 Pa (see Fig. 2). At this pressure value, sublimation begins - the removal of moisture from the frozen product by evaporating it in a vacuum, bypassing the liquid phase (see Fig. 2). Latent heat H during sublimation is spent on the phase transition of ice into steam. The product temperature increases due to the supply of heat to the bottom surface and the side surface of the tray. Heating also occurs due to thermal radiation from the metal surface of the upper tray.

As a result of thermal heating, the process accelerates and the sublimation front moves across the frozen zone from top to bottom until the process is completely completed.

3. Mathematical model of the sublimation process

Frozen milk was presented as a fine-pored body in which the skeleton of the body is the dried product, and the intrapore space is filled with ice, which carries out the interphase transition during the drying process [18,19].

Modeling of the ice sublimation process is considered as a Stefan problem with a moving front, which is the interface between the frozen and dried zones (see Fig. 3).

The temperature distribution in the dried and frozen zone of the product is described by the equations:

$$\rho_d C_d \frac{\partial T}{\partial t} + \rho_v C_v u \bullet \nabla T = \nabla(k_d \nabla T) \tag{1}$$

$$\rho_f C_f \frac{\partial T}{\partial t} = \nabla(k_f \nabla T) \tag{2}$$

where T is the absolute temperature; ρ_d, C_d, k_d and ρ_f, C_f, k_f are the values of density, specific heat capacity, thermal conductivity of the dried and frozen zones of the product, respectively; ρ_v, C_v are the values of density and specific heat capacity of steam.

The distribution of vapor density ρ_v in the dried zone of the product is described by the mass balance equation taking into account the processes of convection and diffusion of vapor:

$$\varphi \frac{\partial \rho_v}{\partial t} + \nabla(\rho_v \boldsymbol{u}) = \varphi \nabla(\Gamma_v \nabla \rho_v) \tag{3}$$

where φ is the value of the porosity of the dried residue; $\boldsymbol{u}$ is the vector of steam movement velocities, Γ_v is the steam diffusion coefficient, which is determined by the following relationship

$$\Gamma_v = \frac{78.5 \bullet 10^{-4}}{3.4 + \frac{P}{133.3}}$$

where P is the absolute vapor pressure.

Since the movement of steam occurs in a porous medium, the velocity vector u is found using the well-known Darcy's law:

$$\boldsymbol{u} = -\frac{K}{\eta_v} \nabla P \tag{4}$$

where K is the permeability coefficient of the product, η_v is the dynamic viscosity of the vapor, which is determined by the relationship:

$$\eta_v = \frac{0.11 \left(\frac{T}{273.15}\right)^{1.5}}{T + 961}$$

The temperature conjugation at the interface between the dried and frozen parts of the product is determined by the Stefan conditions:

$$T|_{B(t)}^{-} = T|_{B(t)}^{+} = T_{sub},$$

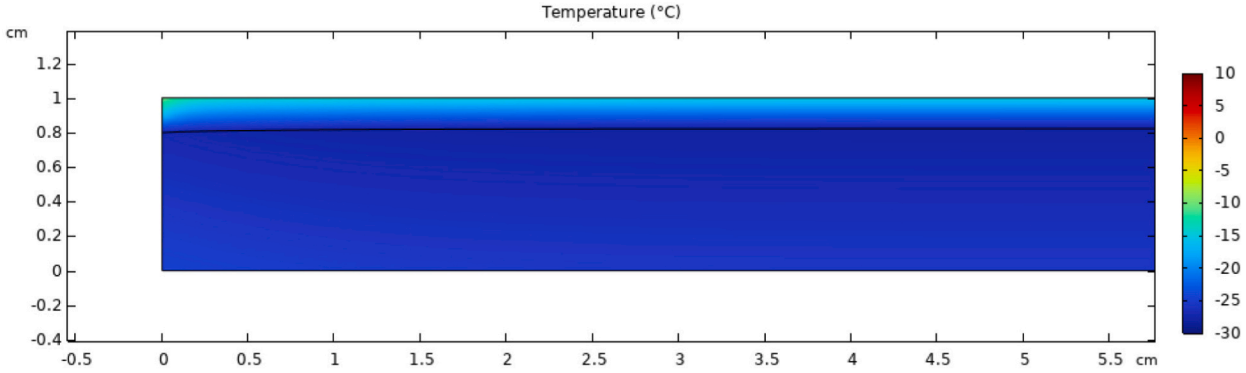
$$k_f \nabla T|_{B(t)}^{+} - k_d \nabla T|_{B(t)}^{-} = \frac{\partial B(t)}{\partial t} (\rho_f - \rho_d) \Delta H \tag{5}$$

where T_{sub} is the temperature of ice at the ice-gas front at which its sublimation into steam occurs; B(t) is the location of the sublimation front in space; ΔH is the latent heat (energy) of sublimation. The value of the vapor density at the sublimation front is described by the following condition:

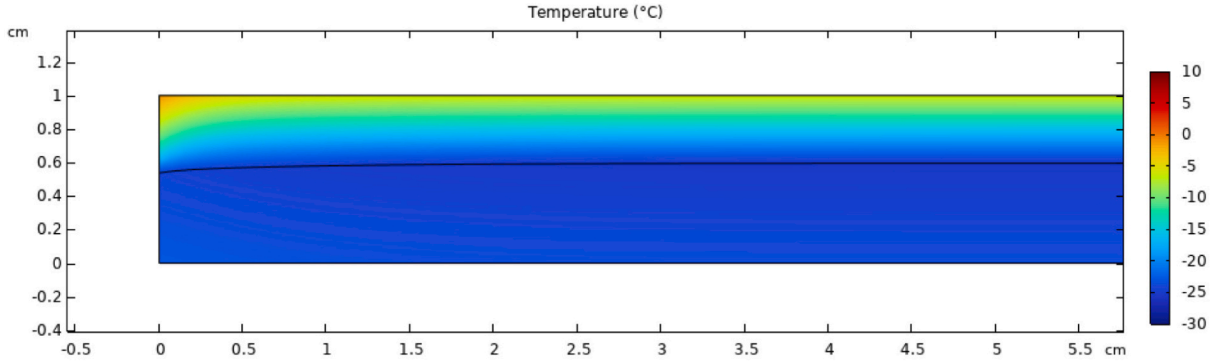
$$\rho_v u|_{B(t)}^{-} = -\rho_v \frac{K}{\eta_v} \nabla P \Big|_{B(t)}^{-} = \frac{\partial B(t)}{\partial t} (\rho_f - \rho_d) \tag{6}$$

4. Phase field method

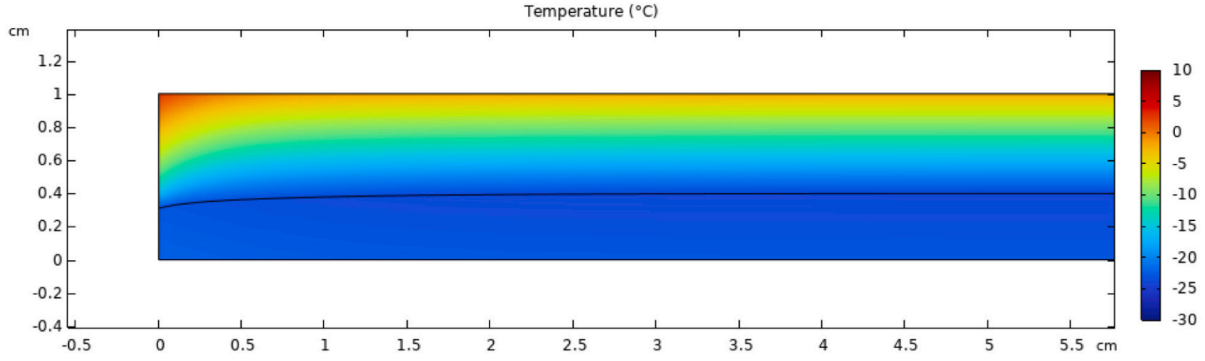
The calculation of the Stefan problem for the milk sublimation



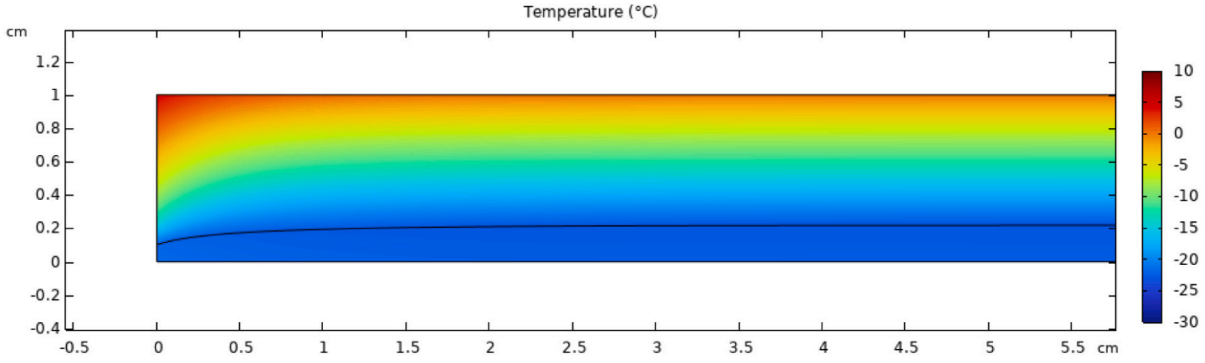
a) 1 hour drying



b) 3 hours drying

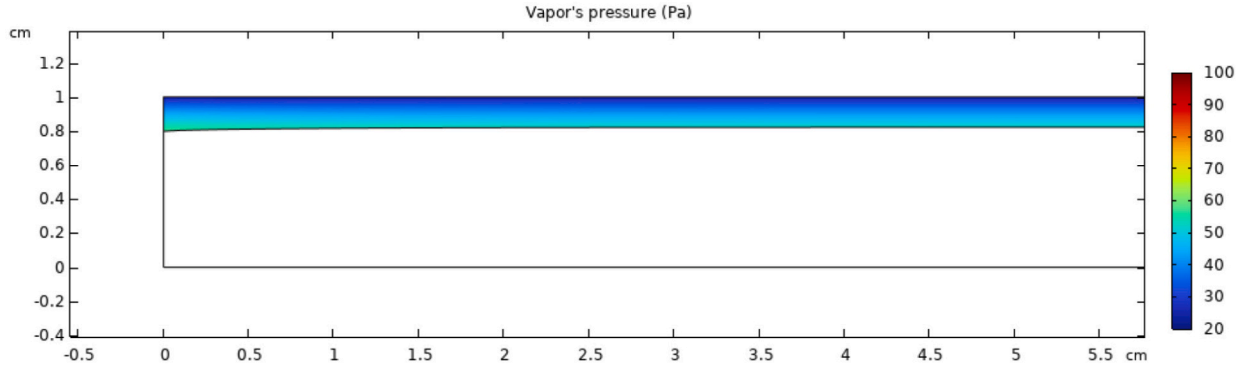


c) 5 hours of drying

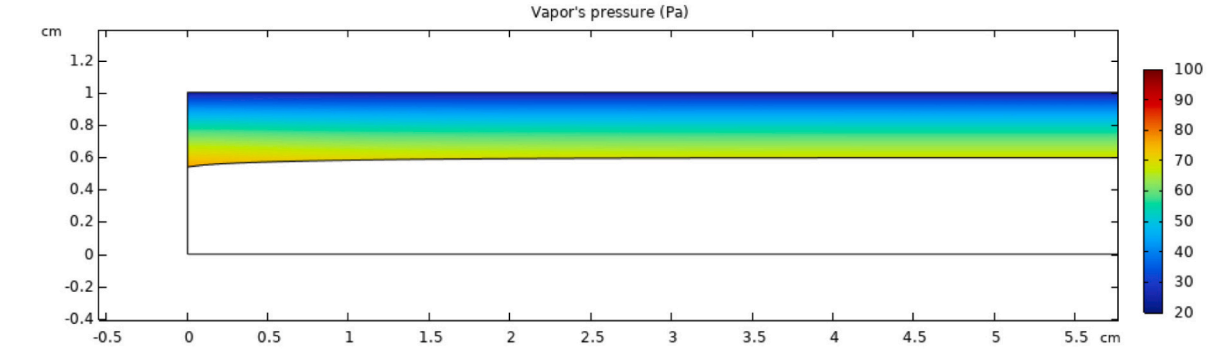


d) 7 hours of drying

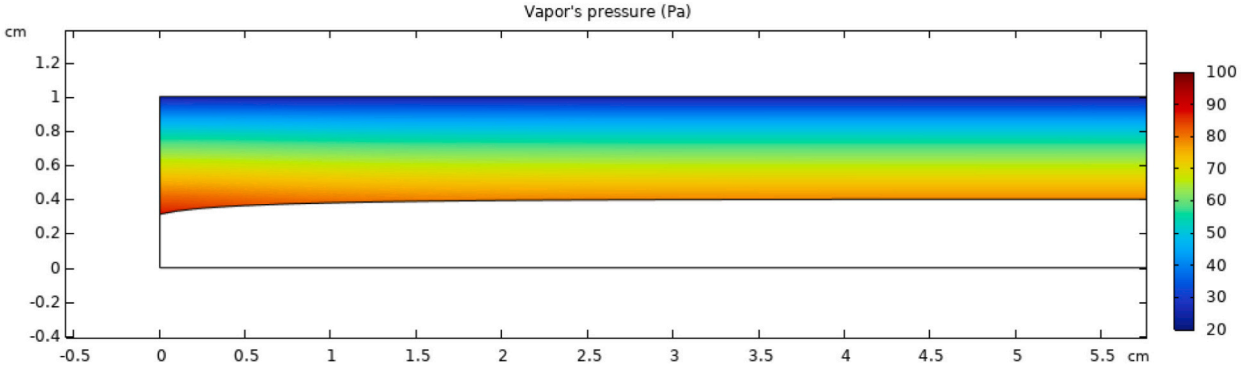
Fig. 5. Distribution of steam temperature over time.



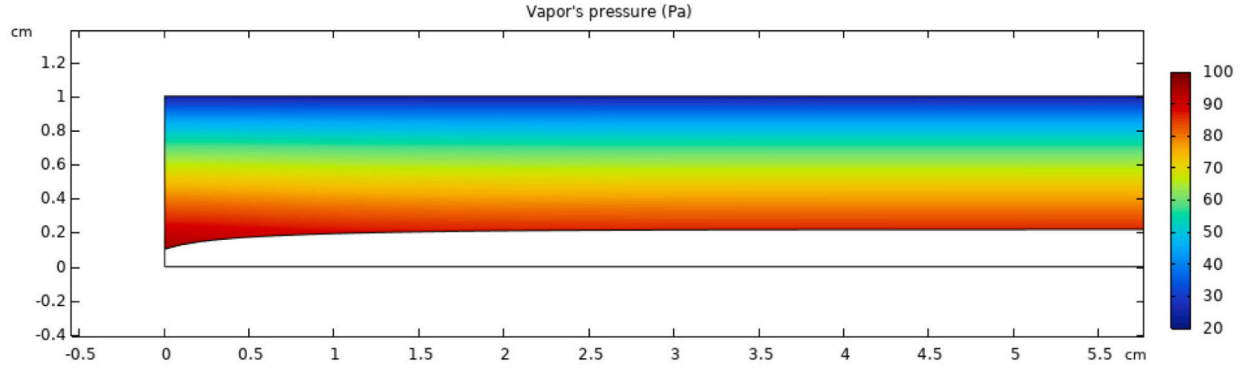
a) 1 hour drying



b) 3 hours drying

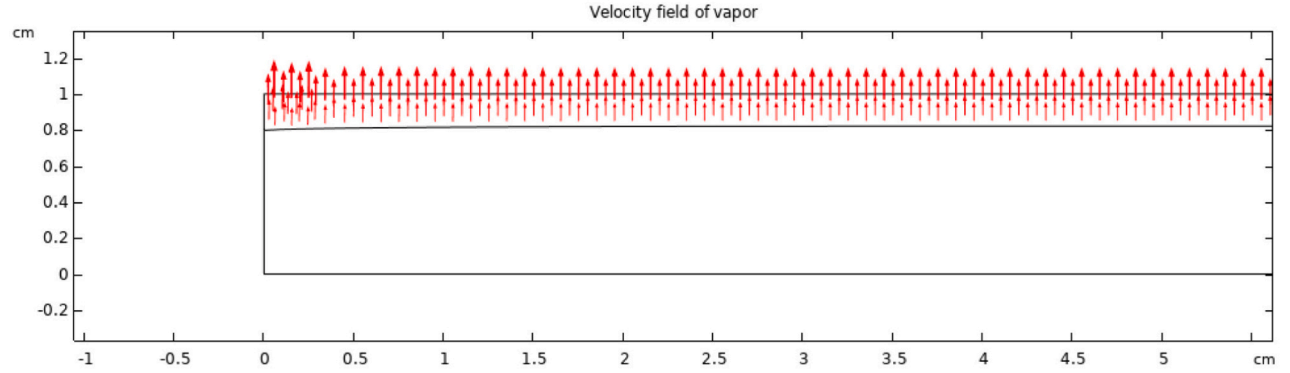


c) 5 hours of drying

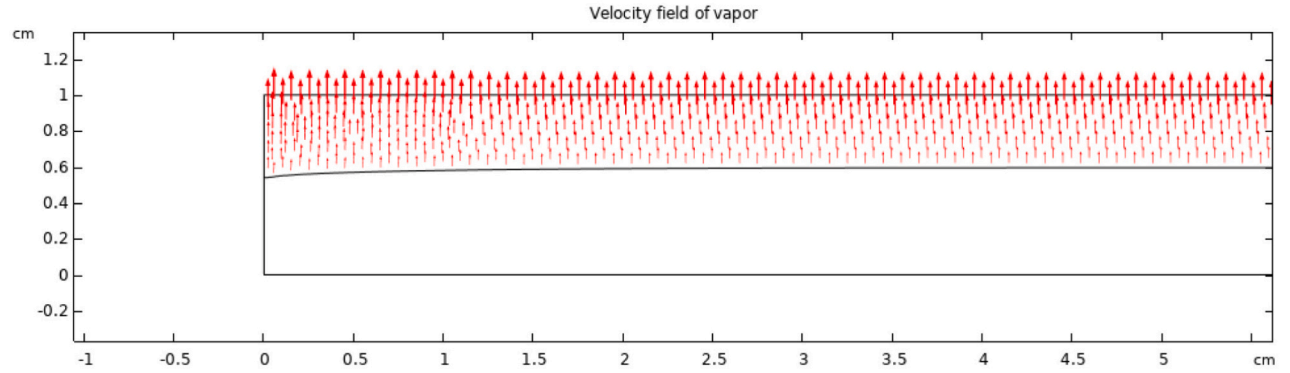


d) 7 hours of drying

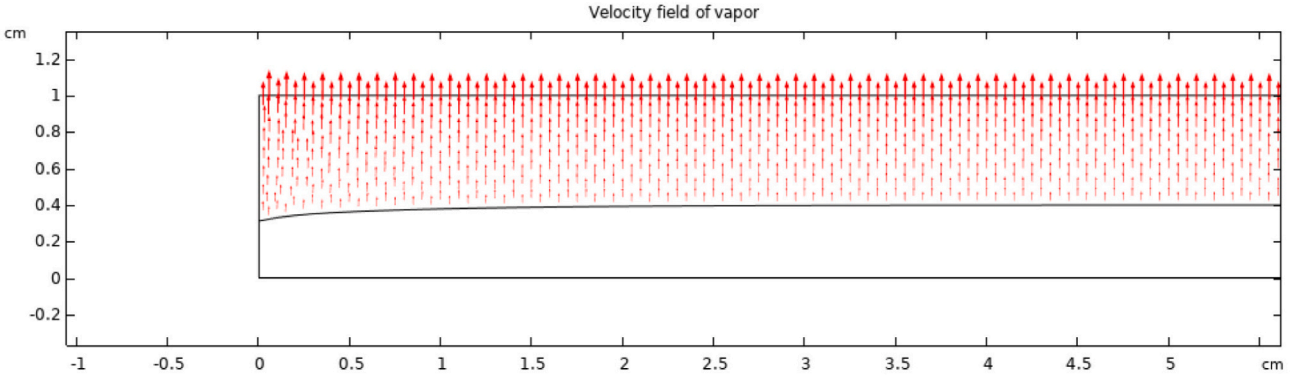
Fig. 6. Distribution of steam pressure over time.



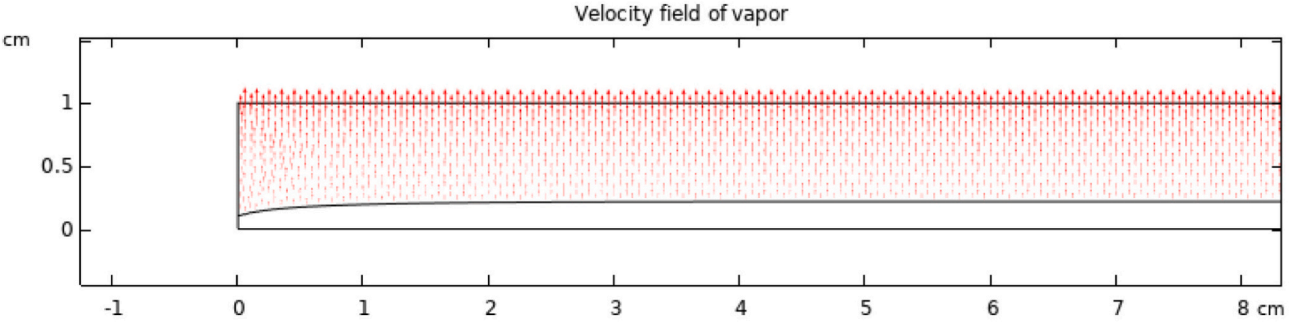
a) 1 hour drying



b) 3 hours drying



c) 5 hours of drying



d) 7 hours of drying

Fig. 7. Steam movement over time (velocity vector scale 0.2).



Fig. 8. Photograph of dried product with cracks.

process is carried out using the phase field method [19], which allows one not to isolate the ice-vapor phase interface and to use the general equation in the entire calculation domain.

Let the dimensionless quantity $\theta = \theta(x,t)$ (having values from 0 to 1) show the relative content of ice in space and time, θ is the phase change in the equations described below.

For each point in space and time, the value θ determines the average values of heat capacity $(\rho C)^{\theta}$ and thermal conductivity k^{θ} [19]:

$$(\rho C)^{\theta} = (1-\varphi)\rho_M C_M + \varphi\theta\rho_I C_I + \varphi(1-\theta)\rho_v C_v \tag{7}$$

$$k^{\theta} = (1-\varphi)k_M + \varphi\theta k_I + \varphi(1-\theta)k_v \tag{8}$$

where φ is the relative water content in milk; ρ_M, C_M, k_M and ρ_I, C_I, k_I are the values of density, specific heat capacity, thermal conductivity of dried residue and ice, respectively; k_v is the thermal conductivity of water vapor. From here, the density values of the frozen and dried zones of the product are determined as follows:

$$\rho_f = \rho_M + \rho_I, \rho_d = \rho_M + \rho_v \approx \rho_M$$

Due to the low density of the vapor compared to the densities of ice and the dried residue of the product ($\rho_v \ll \rho_M$, $\rho_v \ll \rho_I$), it was assumed that the vapor content does not have a noticeable effect on the value of the average heat capacity and on the temperature distribution in the product.

In this regard, the term $\varphi(1\text{-}\theta)\rho_v C_v$ in formula (7) and the convective term $\rho_v C_v \boldsymbol{u}\bullet\nabla T$ in Eq. (1) were excluded.

Using the values of θ, $(\rho C)^{\theta}$, k^{θ}, the equations for temperature (1)–(2) and the conjugation conditions at the sublimation boundary (5) were replaced by a single heat conduction equation for two zones, taking into account the absorption of sublimation heat at the ice-gas front [19]:

$$(\rho C)^{\theta}\frac{\partial T}{\partial t} = \nabla\left(k^{\theta}\nabla T\right) - \frac{\partial\theta}{\partial t}\varphi\rho_I\Delta H \tag{9}$$

The equation for the vapor density ρ_v (3) and the boundary condition at the sublimation surface (6) were replaced by a single equation in the dried or defrosted part of the product ($\theta < 1$) taking into account the formation of vapor during the sublimation of ice [19]:

$$\varphi(1-\theta)\frac{\partial\rho_v}{\partial t} + \nabla(\boldsymbol{u}\rho_v) = \nabla(\varphi(1-\theta)\Gamma_v\nabla\rho_v) - \frac{\partial\theta}{\partial t}\varphi\rho_I \tag{10}$$

For water vapor, the ideal gas model was used, the pressure value of which is determined by the Mendeleev-Clapeyron equation:

$$P = \frac{\rho_v}{M_v}RT \tag{11}$$

where M_v is the molar mass of vapor, R is the universal gas constant.

Note that in reality the value of θ at the sublimation front has a discontinuity: a sharp jump in value between 0 and 1. However, for numerical modeling, it was assumed that this jump is smoothed, using the regulation function [19]:

$$(1-\theta) = \begin{cases} 0, r < -0.5 \\ 6(r+0.5)^5 - 15(r+0.5)^4 + 10(r+0.5)^3, -0.5 \le r \le 0.5 \\ 1, r > 0.5 \end{cases}$$

$$r = \frac{T - T_{sub}}{\Delta T_{sub}} \tag{12}$$

where ΔT_{sub} is the interval of ice temperatures at which ice begins and ends sublimation. In reality, $\Delta T_{sub} = 0$, but in the numerical implementation, $\Delta T_{sub} = 2$ was adopted to smooth out the jump in θ.

The dependence of the ice sublimation temperature on the pressure in the phase contact zone is described by the Clausius-Clapeyron equation:

$$T_{sub} = 2.19 \bullet 10^{-3}\frac{\Delta H}{28.89 - \ln P} \tag{13}$$

5. Boundary and initial conditions

The boundary conditions are formulated for a two-dimensional problem in the following form.

At the bottom and at the left boundary, the product is heated by contact with the metal wall of the tray with a given temperature T_{set}, in connection with which the following conditions were set at the bottom and left boundary of the region:

$$T = T_{set}, u_y = 0 \tag{14}$$

On top of the product, the conditions of an open boundary and heating through thermal radiation are set:

$$n\left(k^{\theta}\nabla T\right) = \varepsilon\sigma\left(T_{set}^4 - T^4\right), P = P_{ch} \tag{15}$$

where n is the unit direction vector; ε is the emissivity of the metal surface; σ is the Stefan-Boltzmann constant; P_{ch} is the pressure in the sublimation drying chamber.

On the right boundary of the calculation domain, the symmetry conditions are set:

$$\frac{\partial T}{\partial x} = 0, \frac{\partial P}{\partial x} = 0 \tag{16}$$

The initial conditions were given as follows:

$$T(x,y,0) = T_0, \rho_v(x,y,0) = \frac{P_{ch}M_v}{RT_0} \tag{17}$$

where T_0 is the temperature of the product before the start of sublimation drying.

Thus, the phase field method allows us to solve the problem by end-to-end calculation, numerically solving the system of Eqs. (4), (9)–(13), taking into account the initial and boundary conditions (14)–(17).

6. Numerical implementation

As can be seen from expressions (4), (7)–(13), the variables $\boldsymbol{u}$,T,θ, P,ρ_v,T_{sub} are interdependent. Differential Eqs. (9)–(10) are nonlinear. This nonlinearity is taken into account by a time cycle for the convergence of the variables $\boldsymbol{u}$,T,θ,P,ρ_v,T_{sub} using the under-relaxation method. The equations for the temperature and vapor density (9)–(10) are approximated using the finite volume method in five-point implicit schemes. The five-point implicit schemes for (9)–(10) determined the type of SLAEs, which were solved using a combination of the alternating direction method and the sweep method. A staggered grid was used in the calculations (Fig. 4), in which the velocity vector components are calculated on the faces of finite volumes.

The boundaries of the computational region coincide with the faces

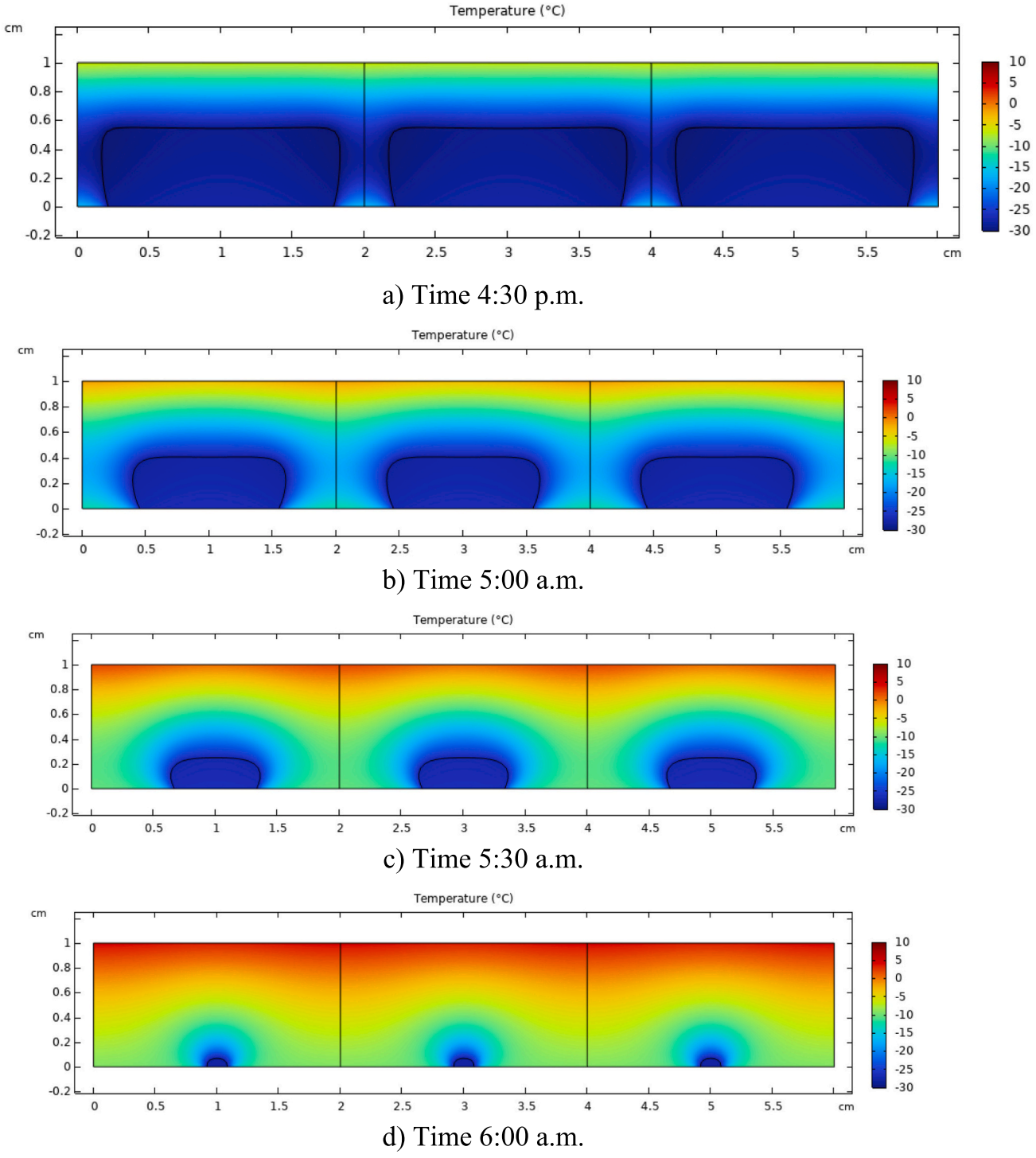


Fig. 9. Distribution of steam temperature over time.

of the boundary cells. The derivatives for the diffusion fluxes on all cell faces (including the boundary ones) were approximated by a second-order scheme. For the convective terms of Eq. (10), the central scheme was used, since with the input parameters used, the Peclet number in modulus is significantly less than 1 (there was a clear predominance of diffusion over convection).

7. Simulation results

The calculations were performed at a constant sublimation temperature $T_{sub} = -40$ °C with the following initial data: the size of the dried product is 0.7 cm × 40 cm (the size of the calculated area is 0.7 × 20 cm). Heating from above occurs by thermal radiation of the metal with a temperature of 10 °C; heating from below and from the side by thermal conductivity with the metal; the initial temperature of the product is −40 °C; the pressure in the drying chamber is 24 Pa; the porosity of the dried product is 0.709.

Table 1 shows the operating parameters for modeling the freeze-drying process. The calculations used parameters of dried and frozen zones of skim mare's milk. The parameters are obtained from [2,20,21]

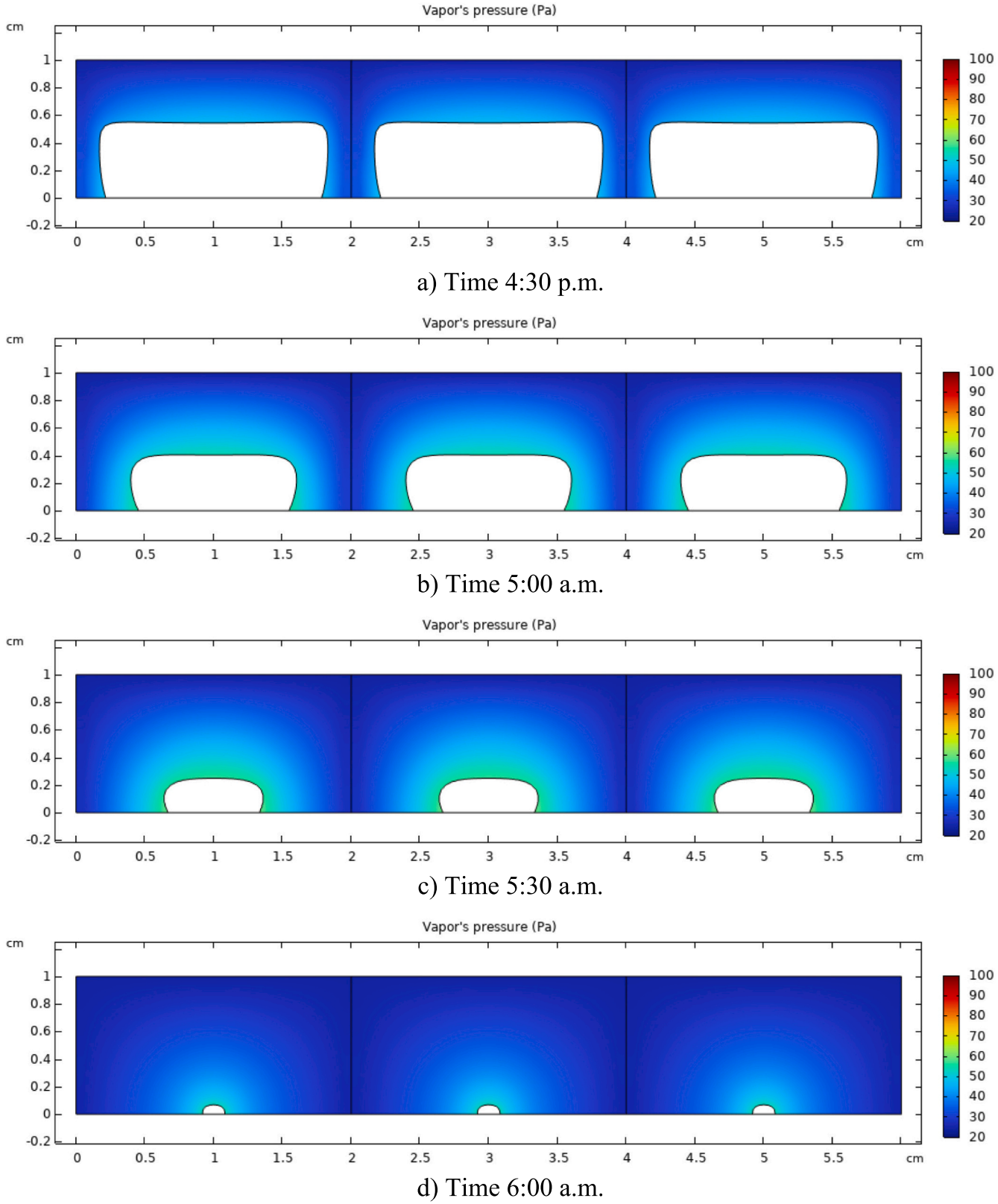


Fig. 10. Distribution of steam pressure over time.

and correspond to skim milk.

Fig. 5 shows the calculations of the temperature distribution in the calculation area without a crack at different moments in time (1 h, 2 h, 5 h, 7 h). Temperature color palette: red – 10 °C, blue – -30 °C.

As can be seen from Fig. 5, the sublimation front moves from top to bottom, as in [17–19]. It is known that the porous structure in contact with the wall has a higher permeability than in the rest of its part. Therefore, the speed of sublimation front movement on the left

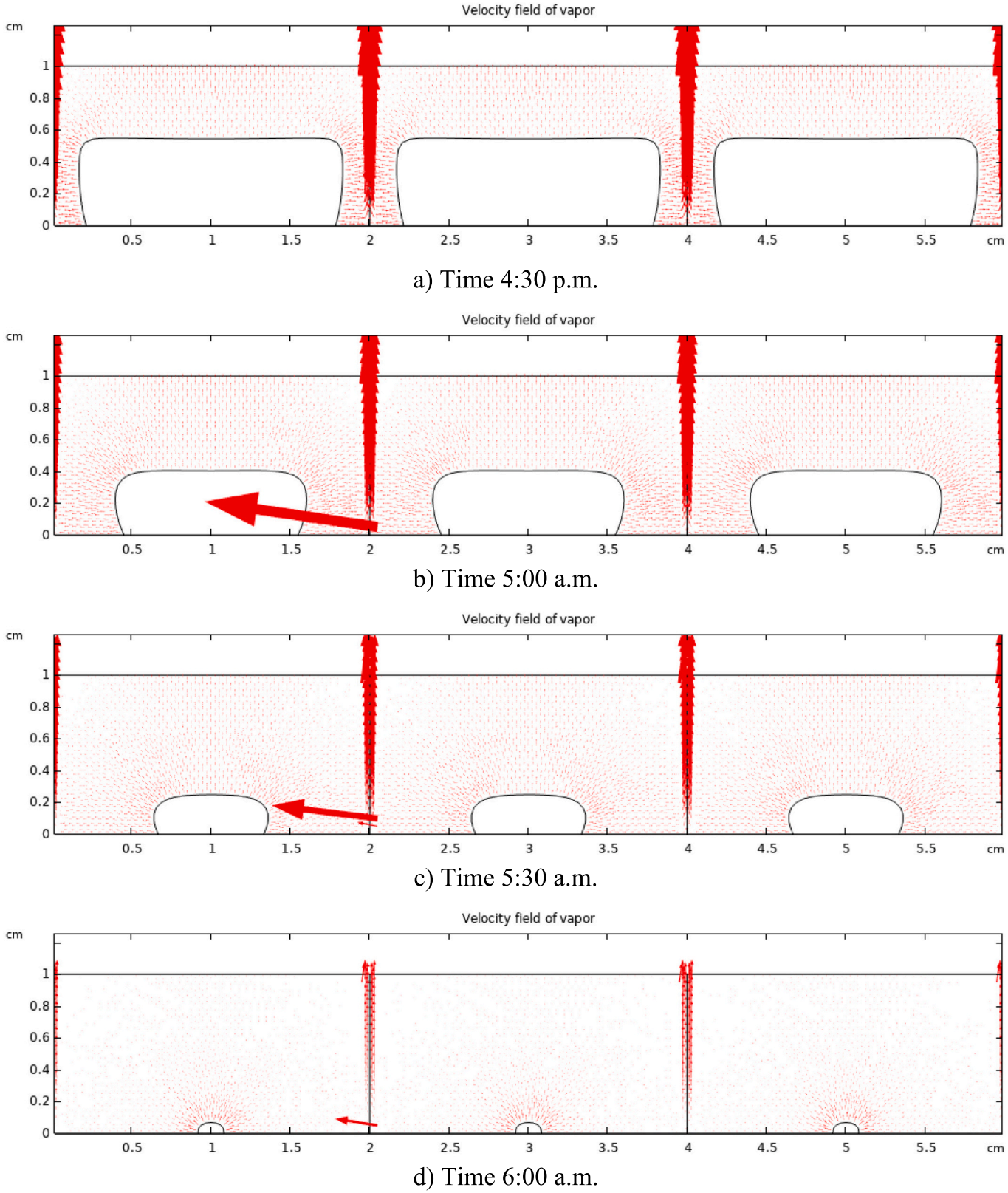


Fig. 11. Steam movement over time (velocity vector scale 0.1)

boundary is somewhat higher (see Fig. 5). Fig. 6 shows the vapor pressure distributions. The color palette of vapor pressure: red - 100 Pa, blue - 20 Pa.

As can be seen from Fig. 6, the vapor pressure has a maximum value at the bottom of the calculation region. The pressure difference is 80 Pa and is explained by the release of steam at the sublimation front into the chamber through the porous structure of the dried product.

Fig. 7 shows the speeds of vapor movement in the porous structure.

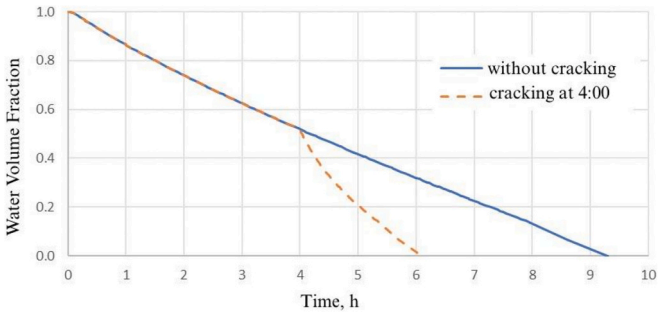


Fig. 12. Change in the volume fraction of water over time with and without taking into account cracks.

At first, steam comes out of the upper part due to sublimation, then as the sublimation front advances, steam begins to gradually come out of the remaining part of the frozen zone. From the distribution pattern of the steam movement, one can see the spread of the sublimation front in the porous structure of the product. These figures also show that the speed of steam movement is somewhat higher at the left boundary due to the high permeability of the porous structure of the product near the side wall (see Fig. 7).

In the experiments, a dried product with cracks was obtained [18] (see Fig. 8).

In this regard, the second series of calculations was carried out taking into account the cracking of the product at the time of 4:00 h. and taking into account the change in the permeability of the porous body during crack formation (see Fig. 9–11).

Cracks were formed every 2 cm with a thickness of 2 mm. As can be seen from Figs. 9, 10, the presence of cracks divides the sublimation front configuration into parts. Cracks create highly permeable structures, lead to a decrease in pressure at the sublimation front and an acceleration of the vapor release from the porous body of the product.

Complete drying of the product was achieved in 6.1 hours.

Comparing the results of the sublimation process with and without cracks, the following differences can be noted:

1) The sublimation front changes noticeably: when cracks form in the product, the front breaks down into semi-independent drying zones;
2) Without crack formation, as the dried zone moves deeper into the product, the pressure at the sublimation front increases significantly (see Fig. 6). When cracks form, the pressure at the sublimation front decreases significantly (see Fig. 10), which can be the cause of cracking.
3) Each crack serves as a powerful “steam drain” (see Fig. 11): the speed of steam movement through cracks is 2 orders of magnitude higher than in the pores of the product. Each crack also draws in steam in the pores of the dried product located in its vicinity. Thus, crack formation significantly reduces the drying time of the product (see Fig. 12).

In practice, the milk drying time is longer than calculations with a constant sublimation temperature show, but shorter than calculations with a variable T_{sub} show. The fact is that when modeling the process of heating the product and sublimation of ice, a constant porous structure of the product is considered. In reality, at some point during drying, cracking of the product occurs. In this case, excess steam can quickly leave the porous body of the product, thereby significantly reducing the pressure of the remaining steam and, as a result, the sublimation temperature of milk ice will drop and lead to an acceleration of the drying process.

8. Conclusion

In a two-dimensional formulation of the problem, calculations were performed at a constant sublimation temperature $T_{sub} = -40$ °C with the following initial data: the size of the product for sublimation is 0.7 cm × 40 cm (the size of the calculation area is 0.7 × 20 cm); heating from above by thermal radiation of the metal with a temperature of 10 °C; heating from below and from the side by thermal conductivity with the metal; the initial temperature of the product is −40 °C; the pressure in the drying chamber is 24 Pa; the porosity of the drying product is 0.709.

Modeling of the ice sublimation process is considered as a Stefan problem with a moving front, which is the interface between the frozen and dried zones. For numerical implementation, the finite volume method with an adaptive grid was used. The calculations took into account the dependence of the phase transition temperature of ice on the pressure at the sublimation front.

Comparative two series of calculations of sublimation drying with initial parameters with and without a crack in the porous medium of the product were carried out. The calculated data showed that cracks lead to an acceleration of the process of sublimation drying of mare’s milk.

The process of crack formation depends on the properties of the stress-strain body of the dry milk residue (Young’s modulus, Poisson’s ratio, critical rupture stress, etc.), which depend on the composition of milk. In this regard, the analysis and determination of the values of crack distribution density, their thickness and critical pressure (at the sublimation front) for cracking of the product requires further research.

CRediT authorship contribution statement

Timur Bekibayev: Visualization, Software, Methodology. **Uzak Zhapbasbayev:** Writing – review & editing, Methodology, Conceptualization. **Nurbibi Imanbayeva:** Writing – review & editing, Visualization, Conceptualization. **Ayaulym Rakhmatulina:** Visualization.

Funding

This research is funded by the Committee of Science of the Ministry of Science and Higher Education of the Republic of Kazakhstan (Grant No. BR21881957).

Declaration of competing interest

The authors declare that they have no known competing financial interests or personal relationships that could have appeared to influence the work reported in this paper.

Data availability

Data will be made available on request.

References

[1] D.P. Lebedev, B.N. Bykhovskii, Mathematical modeling of the process of sublimation drying, J. Eng. Phys. Thermophys. 79 (2006) 48–56, https://doi.org/10.1007/s10891-006-0065-6.
[2] R. Naik, G. Arunsandeep, V.P. Chandramohan, Numerical simulation for freeze drying of skimmed Milk with moving sublimation front using tri-diagonal matrix algorithm, J. Appl. Fluid Mechan. 10 (2017) 813–818, https://doi.org/10.18869/acadpub.jafm.73.240.27054.
[3] A.D. Warning, J.M.R. Arquiza, A.K. Datta, A multiphase porous medium transport model with distributed sublimation front to simulate vacuum freeze drying, Food Bioprod. Process. 94 (2015) 637–648, https://doi.org/10.1016/j.fbp.2014.08.011.
[4] V. Kshirsagar, S. Tchessalov, F. Kanka, D. Hiebert, A. Alexeenko, Determining maximum sublimation rate for a production Lyophilizer: computational modeling and comparison with ice slab tests, J. Pharm. Sci. 108 (2019) 382–390.
[5] K. Nakagawa, Mathematical modeling of freeze-drying process, in: Freeze Drying of Food Products, 2024, https://doi.org/10.1002/9781119982098.ch (eds R.B. Waghmare, M. Kumar and P.S. Panesar).
[6] V. Chaurasiya, Numerical simulation of a non-linear sublimation process with temperature-dependent permeability and volumetric heat source: a phase change problem, Comput. Math. Appl. 176 (2024) 55–66.
[7] K. Nakagawa, T. Ochiai, A mathematical model of multi-dimensional freeze-drying for food products, J. Food Eng. 161 (2015) 55–67.

[8] J.K.N. Rai, J. Singh, An analytical study on sublimation process in the presence of convection effect with heat and mass transfer in porous medium, Int. Commun. Heat Mass Transf. 131 (2022) 105833, https://doi.org/10.1016/j.icheatmasstransfer.2021.105833.
[9] V. Chaurasiya, J. Singh, An analytical study of coupled convective heat and mass transfer with volumetric heating describing sublimation of a porous body under most sensitive temperature inputs: application of freeze-drying, Int. J. Heat Mass Transf. 214 (2023) 12429, https://doi.org/10.1016/j.ijheatmasstransfer.2023.124294.
[10] E.A. Boss, R.M. Filho, E.C. Vasco de Toledo, Freeze drying process: real time model and optimization, Chem. Eng. Process. Process Intensif. 43 (12) (2004) 1475–1485, https://doi.org/10.1016/j.cep.2004.01.005.
[11] E. Mokhova, M. Gordienko, N. Menshutina, Mathematical model of freeze drying taking into account uneven heat and mass transfer over the volume of the working chamber, Dry. Technol. 40 (12) (2022) 2470–2493, https://doi.org/10.1080/07373937.2022.2058958.
[12] A.A. Barresi, V. Rasetto, D.L. Marchisio, Use of computational fluid dynamics for improving freeze-dryers design and process understanding. Part 1: modelling the lyophilisation chamber, Eur. J. Pharm. Biopharm. 129 (2018) 30–44, https://doi.org/10.1016/j.ejpb.2018.05.008.
[13] A.A. Barresi, D.L. Marchis, Computational fluid dynamics data for improving freeze-dryers design, Data Brief 19 (2018) 1181–1213, https://doi.org/10.1016/j.ejpb.2018.05.008.
[14] Y. Liu, Y. Zhao, X. Feng, Exergy analysis for a freeze-drying process, Appl. Therm. Eng. 28 (7) (2008) 675–690, https://doi.org/10.1016/j.applthermaleng.2007.06.004.
[15] M. Reitzle, S. Ruberto, R. Stierle, J. Gross, T. Janzen, B. Weigand, Direct numerical simulation of sublimating ice particles, Int. J. Therm. Sci. 145 (2019), https://doi.org/10.1016/j.ijthermalsci.2019.05.009.
[16] R. Pisano, Achieving continuous manufacturing in lyophilization: technologies and approaches, Eur. J. Pharm. Biopharm. 142 (2019) 265–279, https://doi.org/10.1016/j.ejpb.2019.06.027.
[17] B.L. Chen, J.H. Jang, M. Amani, W.M. Yan, Numerical and experimental study on the heat and mass transfer of kiwifruit during vacuum freeze-drying process, Alex. Eng. J. 73 (2023) 427–442.
[18] A. Rakhmatulina, A. Altybay, N. Imanbayeva, S. Bagitova, A. Baikonys, Numerical simulation and experimental analysis of Mare's Milk sublimation drying, Processes 13 (2025) 206, https://doi.org/10.3390/pr13010206.
[19] W.M. El-Maghlany, A. El-R Bedir, M. Elhelw, A. Attia, Freeze-drying modeling via multi-phase porous media transport model, Int. J. Therm. Sci. 135 (2019) 509–522, https://doi.org/10.1016/j.ijthermalsci.2018.10.001.
[20] W.J. Mascarenhas, H.U. Akay, M.J. Pikal, A computational model for finite element analysis of the freeze drying process, Comput. Methods Appl. Mech. Eng. 148 (1997) 105–124, https://doi.org/10.1016/S0045-7825(96)00078-3.
[21] G. Srinivasan, M. Muneeshwaran, B. Raja, Numerical investigation of heat and mass transfer behavior of freeze drying of Milk in vial, Heat Mass Transf. 55 (2019) 2073–2081, https://doi.org/10.1007/s00231-018-02538-1.